pubs.acs.org/Biomac

Article

Fabrication of Low-Temperature Fast Gelation β-Cyclodextrin-Based Hydrogel-Loaded Medicine for Wound Dressings

Juanli Shen, Shiyu Fu,* Xiaohong Liu, Shenglong Tian, Detao Liu, and Hao Liu

Cite This: https://doi.org/10.1021/acs.biomac.3c00708

Read Online

ACCESS | Metrics & More | Article Recommendations | Supporting Information

ABSTRACT: β-Cyclodextrin (β-CD) is often used as a drug carrier for biomedical materials due to its unique cavity structure. Herein, β-CD was modified by acryloyl chloride and further copolymerized with *N*-isopropylacrylamide (NIPAM) and acrylic acid (AA) to obtain PNIPAM-*co*-β-CD-AC. The results showed that the critical phase transition temperature of PNIPAM/β-CD-AC could be controlled at 19 °C, and the fast sol−gel phase transition was realized in 2−10 s. The hydrophobic drug carried in this hydrogel can constantly be released for more than 6 days at pH values (pH 5.5−8), and the duration may match the recovery of the wound. As a dressing hydrogel, its rapid gel formation and inversion as well as shear-thinning behavior prevent secondary wound damage. The β-CD-based hydrogel also has good biocompatibility and antioxidant properties, which provide a good potential choice for wound dressings, especially for exposed wounds in winter.

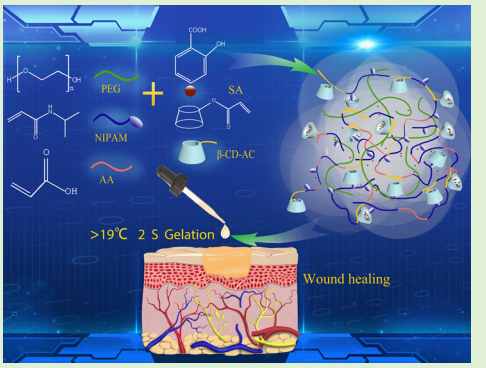

1. INTRODUCTION

Polysaccharides obtained from biomass are often applied to manufacture medical materials with biocompatibility and environmental friendliness. β-Cyclodextrin (β-CD) is a special carbohydrate polymer, derived from starch with a ring constructed with 7 glucose units, which provides a cavity to bind or chelate some chemicals.[1] The cavity of β-CD provides the possibility of loading or releasing hydrophobic drugs. Due to its special structure and large number of functional groups, β-CD possesses the adsorption sites and many oxygen-containing functional groups.[2] As a result, a variety of hydrophobic small molecule drugs form inclusion complexes with β-CD through reversible host−guest interactions.[3,4] The solubility and stability of these guest molecules are further improved. More interestingly, the host−guest package formed by cyclodextrins and small molecule drugs can control the release of the drug, thus preventing adverse reactions caused by a rapid release of the drug.[5] Anyway, for original β-CD, there are some shortages, such as poor water solubility and low binding stability.[6]

To obtain stronger water solubility and the function to control the carrying substances, β-CD is usually modified by grafting polymers with special functions on the hydroxy group.[7] The modified β-CD became a hydrogel with thermo-response when grafted PNIPAM on its ring.[8] β-CD embedded into chitosan/αβ-phosphate can form a thermosensitive hydrogel for medicine delivery.[9] Although it is not possible to strictly distinguish whether the drug molecules are present in the polymer chains of the gel or the β-CD cavities, the bulk of the early rapid release of the drug comes from the free drug molecules in the polymer network, and the sustained release in the later stages is mainly controlled by the guest−host interactions of β-CD with the drug.[3] As the external environment changes (temperature, pH, and external solution concentration), hydrogels respond to external stimuli, thereby affecting the rate of slow drug release.[10] For example, when the temperature is above the lower critical solution temperature (LCST), the PNIPAM polymer chains shrink causing a squeezing effect; when the temperature is increased to temperatures above the lower critical solution temperature, the hydrogel will exhibit rapid swelling kinetics, and all of these motions can release the drug from the drug-loaded hydrogel.[11] However, the β-CD inclusion complex in the hydrogel is liable to be lost because of the weak physical cross-linking in a hydrogel, which affects the efficiency of drug release. To improve the strength of cross-linking of the hydrogel, β-CD is often modified with grafted polymer or copolymers. The hydroxyl groups on β-cyclodextrin provide sites for grafting reaction to fabricate β-CD functional materials with suitable water solubility, surface activity, and water absorption.[12] The derivatives of β-CD with grafted NIPAM formed stable chemical cross-linking to enhance the mechanical strength of the gel. Yu et al.[13] selected acryloyl-β-cyclodextrin (β-CD-AC) as the host molecules to form the hydrogel network for improving the solubility of cyclodextrin. The graphene oxide/

Received: July 18, 2023
Revised: October 1, 2023
Accepted: October 2, 2023

poly(*N*-isopropylacrylamide-*co*-*β*-cyclodextrin) composite is a thermosensitive hydrogel because vinyl functional groups were introduced on *β*-CD and copolymerized with NIPAM.[14] The vinyl group grafted on *β*-CD is crucial to the cross-linking of the copolymers in the gel.

The modified *β*-CD-based hydrogel has the potential to be applied in dressing for wound repair, in which the modified *β*-CD acts as a drug carrier that can controllably release drugs stimulated by the grafted responsive functional copolymer. These wound dressings will be better than the traditional dressing materials, such as absorbent cotton gauze, cotton pads, and gauze, which may cause secondary damage or wound infection when changing the dressing materials,[13,15] especially for deep and irregular wounds.[16] Coped with such a question, various artificial skins and wound dressing hydrogels have been developed[17] with three-dimensional porous structure, hydrophiles, and good performance in the absorption of blood and tissue exudates with minimal absorption of proteins from body fluids.[18] The dressing hydrogel can also provide an enough moist environment for wound healing.[19,20]

As mentioned before, the changing of the dressing hydrogel on the wound may cause a secondary injury. Therefore, it is supposed that the hydrogel should bind tightly to irregular wounds to reduce microbial penetration and be easily removed on demand. Sol−gel-transformed hydrogels are proposed to attract many researchers for wound dressing materials.[21] Among them, thermosensitive gels are special in dressings, which respond to an environmental temperature at a critical transition temperature[22] and make the dressing hydrogels easy to bandage and remove.[19,23] PNIPAM is a well-known polymer for temperature-sensitive hydrogel in the biomedical field.[24] The low critical solution temperature (LCST) of poly(*N*-isopropylacrylamide) (PNIPAM) is 32 °C, close to human body temperature.[25] However, the response rate of routine PNIPAM to the temperature is very slow. Furthermore, the LCST at 32 °C is not good in winter for the dressing because the temperature of the exposed skin (face and hands) may be much lower than 32 °C. The low temperature causes the gel to turn into a liquid to loosen the dressing, which is not conducive to wound healing.

In the present paper, a thermosensitive dressing hydrogel at low temperatures was prepared by copolymerization of NIPAM and acrylic acid (AA) on *β*-CD-AC, in which *β*-CD-AC provided the carbon−carbon double bonds copolymerized with the carbon−carbon double bonds of NIPAM or AA to form a copolymer chain. The *β*-CD in the copolymer provides a drug-loaded core and cross-linking points.[26] As mentioned by Ahmet,[27] when the molecules with steric hindrances and hydrophobic structure were applied to prepare hydrogels with NIPAM, the volume phase transition temperature was lower. The hydrophobic functional groups in a polymer can further lower the LCST of the derived gel. The poly(acrylic acid) (PAA) introduced into the gel acts as both a pH response group and an interpenetrating network linker.[28] The critical phase transition rate is accelerated after the copolymerization of NIPAM with hydrophilic monomers (AA). Finally, poly(ethylene glycol) (PEG) was physically introduced to enhance the mechanical strength of the gel and adjust its pore size.[7,29] The gel can cover irregular wounds well and stably release drugs, which may provide the potential for application in the wound healing process.

2. MATERIALS AND METHODS

2.1. Materials. All reagents used were analytical grade and were not further purified. *β*-Cyclodextrin(*β*-CD), acryloyl chloride (AC), ammonium persulfate (APS), *N*-isopropylacrylamide (NIPAM), and acrylic acid (AA) were obtained from Shanghai Aladdin Biochemical Technology Co., Ltd. Poly(ethylene glycol) (PEG), salicylic acid (SA), and 2,2-diphenyl-1-picrylhydrazyl (DPPH) were purchased from Shanghai Macklin Biochemical Co., Ltd. A phosphate buffer solution (PBS) was prepared by disodium hydrogen phosphate ($Na_2HPO_4{\cdot}12H_2O$) and sodium dihydrogen phosphate ($NaH_2PO_4{\cdot}2H_2O$). $Na_2HPO_4{\cdot}12H_2O$ was obtained from Guangdong Guanghua Sci-tech Co., Ltd. $NaH_2PO_4{\cdot}2H_2O$ was obtained from Fuchen (Tianjin) Chemical Reagent Co., Ltd. The deionized water was made in the laboratory.

2.2. Synthesis of Acryloyl-*β*-cyclodextrin (*β*-CD-AC). 2.5 g of *β*-CD was dissolved in KOH (35 mL, 1.0 g) solution and soaked in an ice bath immediately. 7.5 mL of acryloyl chloride was added to the *β*-CD/KOH solution with stirring at 40 °C for 6 h. The solution was dripped in alcohol to obtain a white precipitate, which was centrifuged and washed several times with alcohol to obtain dried *β*-CD-AC.

2.3. Synthesis of PNIPAM-*co*-*β*-CD-AC. The *β*-CD-AC was dissolved in 2 mL of PEG solution (20 mg/mL, 2 mL) and heated in an oil bath to 80 °C. To the solution, NIPAM was added under N_2 and stirred for 2 h, and then, AA (100 *μ*L, 2%) and APS (100 *μ*L, 2%) were added for further copolymerization. Table 1 shows the composition of hydrogels obtained from the copolymerization of NIPAM and *β*-CD-AC in different ratios. The control for hydrogels was synthesized with NIPAM and *β*-CD.

Table 1. Composition of Hydrogels

sample name	principal material ratio	reaction times/h
PNIPAM-*co*-*β*-CD-AC	NIPAM/*β*-CD-AC = 1:1	12
PNIPAM-*co*-*β*-CD-AC1	NIPAM/*β*-CD-AC = 1:2	12
PNIPAM-*co*-*β*-CD-AC2	NIPAM/*β*-CD-AC = 2:1	12
PNIPAM/*β*-CD	NIPAM/*β*-CD = 1:1	12

2.4. Characterization. *2.4.1. Nuclear Magnetic Resonance (NMR).* The NMR experiments were performed on a 400 MHz JEOL NMR spectrometer Bruker Avance neo 500 M. Before NMR analysis, all samples were dissolved in DMSO-6 at a 10 mg/mL concentration.

2.4.2. Scanning Electron Microscopy (SEM). The structural morphology of the hydrogels was visualized by a scanning electron microscope. The PNIPAM-*co*-*β*-CD-AC hydrogel sample sheets were freeze-dried. The fracture surfaces of hydrogels were coated with gold and imaged in a SU5000 (Japan) field-emission scanning electron microscope (FESEM) at an accelerating voltage of 10.0 kV.

2.4.3. FTIR Characterization. Hydrogel samples and *β*-CD and *β*-CD derivatives were analyzed using a Fourier transform infrared spectrometer (TENSOR 27, BRUKER OPTICS Co Ltd.). The hydrogel samples were dried in a freezer at −56 °C for 48 h. Powdered models were mixed with KBr powder compressed for testing and scanning (4000−400 cm^{-1}) at a resolution of 4 cm^{-1}.

2.4.4. Rheological Analysis. Rheological measurements of various PNIPAM-*co*-*β*-CD-AC hydrogel formulations were carried out by using an Anton Paar Physica MCR 302 rheometer. The hydrogel samples were placed between parallel plates of 25 mm diameter and with a gap of 1 mm in oscillatory mode at 37 °C. The storage modulus (G') and loss modulus (G'') were recorded as functions of time. The frequency sweep shows the variation of G' and G'' of the composite hydrogels with frequency (0.1−100 rad s^{-1}) at constant strain (1%). The strain sweep represents the variation of G' and G'' of the composite hydrogels with strain (1−200%) at a constant frequency (1 Hz).

2.4.5. X-ray Photoelectron Spectroscopy (XPS). X-ray photoelectron spectroscopy was performed to determine the *β*-CD-AC and PNIPAM-*co*-*β*-CD-AC hydrogel. A Thermo Scientific K-*α* electron energy analyzer working in a binding energy range of 0−1500 eV to

https://doi.org/10.1021/acs.biomac.3c00708
Biomacromolecules XXXX, XXX, XXX−XXX

Scheme 1. Hydrogel Dressing with Low-Temperature Fast Gel Formation

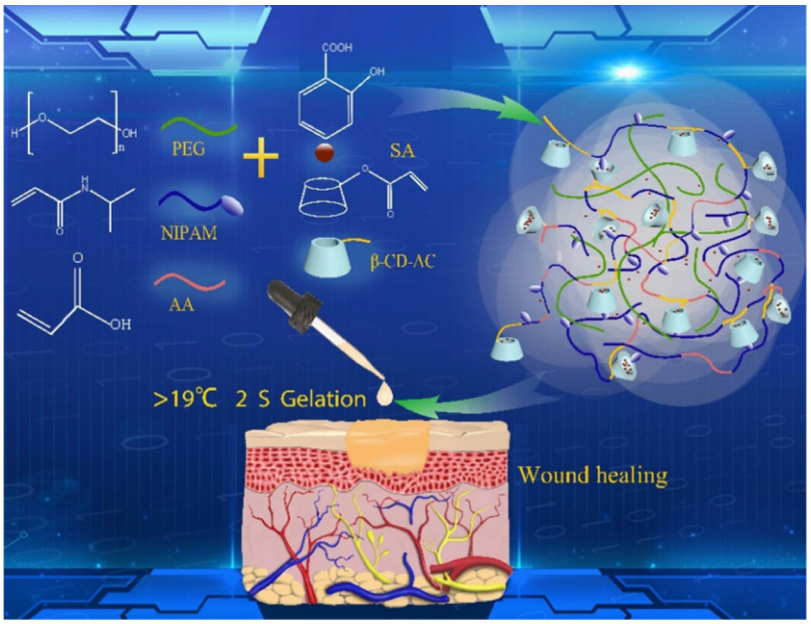

provide precise details regarding the molecular bonds present, elemental composition, and speciation in samples, with an Al Kα monochromatized photon source (photon energy $h\nu$ = 1486.71 eV), was employed at room temperature. The overall energy resolution for XPS measurements was set to 0.5 eV for all of the spectra shown here, and a low-energy flood gun was used (electron energy = 2 eV, beam current = 20 μA).

2.4.6. Thermal Stability (TG). Thermal gravimetric analysis of β-CD, β-CD-AC, NIPAM, and different proportions of PNIPAM-*co*-β-CD-AC hydrogel samples was carried out by using a thermal gravimetric analyzer (SCINCO TGA N-100, Korea). The hydrogel samples were placed in a clean platinum pan and heated from 40 to 800 °C with a heating rate of 10 °C/min under a nitrogen atmosphere.

2.5. Drug Loading and Release In Vitro. The ability of the PNIPAM-*co*-β-CD-AC hydrogels to release drugs under the influence of pH was investigated. Equal amounts of hydrogels were placed in phosphate buffers with different pH values (pH = 5.5, 6.5, 7.4, 8.8, respectively, simulating infection environment and inflammation) to test the drug release effect. The drug sustained release experiment was conducted at different temperatures (25, 30, 35, 37, and 39 °C). Salicylic acid (SA) was selected as the model drug to evaluate the hydrogel's drug loading and the release behaviors from the hydrogel by ultraviolet−visible (UV−vis) spectroscopy (Agilent 8453, Agilent Technologies Co Ltd.).[30] The samples were collected by filtration and centrifugation, and the concentration of SA remaining in the phosphate buffer (pH 7.4, PBS) was determined with UV−vis spectroscopy at a wavelength of 296 nm. Since the β-cyclodextrin-based hydrogel is targeted at the sustained release of hydrophobic drugs, two other hydrophobic drugs (DOX and 5-FU, respectively) are chosen as sustained release under the same conditions (see the Supporting Information for details). At a low temperature (4 °C), 1 mg of the drug was put into 1 mL of a liquid gel for automatic embedding for 12 h. The gel was released in phosphate-buffered saline (PBS) of different variables for about 120 h, and 2.5 mL was extracted each time to measure the drug release. 2.5 mL of blank PBS was put into the experimental group, and three parallel experiments were carried out for each variable group.

2.6. Cytotoxicity Evaluation. CCK-8 method and the Calcein-AM/PI staining method were applied to test the cytotoxicity of hydrogel extracts and evaluate the biocompatibility of hydrogel. After high-temperature sterilization, a certain quality of freeze-dried hydrogel was added to PBS and extracted at 37 °C for 12 h. The extract was added to 10% fetal bovine serum (FBS) and 1% dual antibody to prepare DMEM complete culture medium. Extracts of different concentration gradients were used as the culture medium. Cells without extract were used as the control group. After incubation for 24 h, 100 μL of complete medium containing CCK-8 reagent was added to each well (the volume ratio of CCK-8 reagent to complete medium was 1:9). The cells were rewashed by live/dead cell staining. The survival state was observed with a laser confocal microscope (Leica TCS SP8, Germany). The absorbance of each well at 450 nm was measured with a microplate reader, and the the cell survival rate (CV, %) was calculated by the following formula:

$$\mathrm{CV}(\%) = \frac{A_{\mathrm{sample}}}{A_{\mathrm{control}}} \times 100\% \quad (1)$$

2.7. Antioxidative Activity. The mechanism of antioxidant evaluation is that the 1,1-diphenyl-2-picrylhydrazyl (DPPH) reagent accepts electrons or hydrogen radicals to become a stable molecule. Hydrogen was formed when DPPH reacted with antioxidant agents.[31] The antioxidant properties of hydrogels were evaluated by determining the scavenging ability of hydrogels on DPPH free radicals (nitrogen free radicals and hydroxyl free radicals). The following methods are specified by the scavenging rate of the DPPH free extreme. At first, the 300 μL of hydrogel was immersed in a 1 mL ethanol solution for approximately 1 h. Next, DPPH (100 μL, 0.5 mM) was added to the ethanol solution above and incubated in the dark for 1 h. The control group used the same amount of distilled water instead of the hydrogel. Finally, the absorbance of the ethanol solution was measured spectrophotometrically at 517 nm. The experimental data were obtained by repeating it three times. The scavenging capacity (%) was calculated as

$$\text{scavenging ability } (\%) = \left[1 - \left(\frac{C_{\mathrm{sample}}}{C_{\mathrm{blank}}}\right)\right] \times 100\% \quad (2)$$

2.8. In Vivo Wound Healing Test. Wounds of adult SD mice were treated with the dressing hydrogel to evaluate the healing effect. It was certified by the China Laboratory Animal Certification Association for laboratory animal care.

Mice were fed a standard diet for at least 7 days before the experiment to acclimate to their new environment. SD female mice weighing approximately 200−230 g and 5 weeks old were used in this experiment. They were randomly divided into 2 groups of 3 mice each (n = 3). All mice were anesthetized with sodium pentobarbital (70

https://doi.org/10.1021/acs.biomac.3c00708
Biomacromolecules XXXX, XXX, XXX−XXX

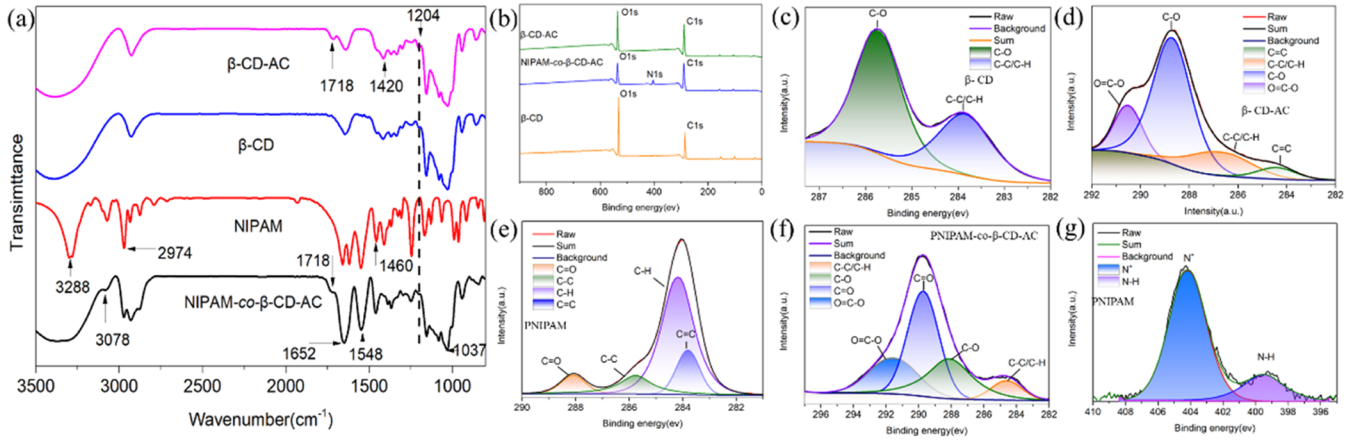

Figure 1. (a) FTIR spectra of *β*-CD-AC, *β*-CD, NIPAM, and PNIPAM-*co*-*β*-CD-AC; (b) XPS spectra of the full scan atlas of NIPAM-co-*β*-CD-AC, *β*-CD, and *β*-CD-AC. (c) high-resolution C 1s XPS peaks of *β*-CD; (d) high-resolution C 1s XPS peaks of *β*-CD-AC; (e) high-resolution C 1s XPS peaks of NIPAM; (f) high-resolution C 1s XPS peaks of PNIPAM-*co*-*β*-CD-AC; and (g) high-resolution N 1s XPS spectra of PNIPAM-*co*-*β*-CD-AC.

mg/kg), their backs were debarked, and the skin was disinfected topically with iodophor. The rats' backs were then incised with a 1.5 cm × 1.5 cm wound at a subcutaneous depth without damaging the fascia or adipose tissue. The thickness of the basal wound was approximately 3 mm.

Two types of hydrogel dressings were covered over the new wound: a blank hydrogel and a drug-laden hydrogel (1.5% SA solution: FuFangHuangBaiYeTuJi = 1:10, mixed drugs/freeze-dried hydrogel = 7:1 g). The dressing was then wrapped in a flexible bandage to prevent detachment. After surgery, the mice lived alone in cages throughout the experiment. All dressings were changed every 2 days.

The time of the first administration was marked as day 0. On days 0, 3, 6, 9, and 12, wound healing was measured, wound size was measured, and photographs were taken according to wound healing. The wound healing rate was calculated by the following formula

$$\text{wound area closure } (\%) = (S_0 - S_n)/S_n \times 100\% \quad (3)$$

where S_0 and S_n are the wound areas on day 0 and at different time points, respectively. The area was calculated on days 0, 3, 6, 9, and 12 using image analysis software for wound photographs.

Rats were executed on day 12 and skin tissue from the wound site (wound and surrounding tissues were excised) was taken for pathological examination. The excised wound portion was promptly fixed in 4% paraformaldehyde, dehydrated, and embedded in paraffin.

3. RESULTS AND DISCUSSION

3.1. Preparation of the PNIPAM-*co*-*β*-CD-AC Hydrogel. *β*-CD is usually implemented to fabricate hydrogels, where it acts as a part of the host−guest cross-linker. However, *β*-CD has a relatively low solubility in water. To gain their solubility and stability in hydrogels, *β*-CD was therefore modified by grafting hydrophilic groups or chains. Herein, *β*-CD was reacted with acryloyl chloride to obtain *β*-CD-AC, in which AC provides a double bond of carbons for subsequent copolymerization (Scheme 1). The infrared (IR) spectra of *β*-CD-AC, *β*-CD, NIPAM, and the copolymer are shown in Figure 1a. In the spectrum of *β*-CD-AC, there are peaks at 1718 and 1204 cm^{-1}, belonging to the carbonyl group and C−O of AC ester linkages, respectively, while there are no peaks in the spectrum of *β*-CD, which indicated that *β*-CD-AC was successfully synthesized. This result is consistent with other literature studies.[32,33] In the PNIPAM-*co*-*β*-CD-AC spectrum, the peaks at 1548, 3078, and 3288 cm^{-1} are corresponded to N−H stretching. The peaks in the range of 3200−3600 cm^{-1} are caused by both N−H and O−H, where the hydroxyl group in *β*-CD. The distribution of hydroxyl groups at the edges of *β*-CD provides an effective adsorption site, a cavity. Thus, SA molecules in an aqueous solution were adsorbed to the edges of the *β*-CD cavity through electrostatic interactions.[34] The peaks at 2974 and 1460 cm^{-1} in the spectrum of NIPAM are caused by asymmetric stretching vibration and asymmetric deformation of N−H. The peak at 1650 cm^{-1} belongs to the first-order amide C═O stretching band in PNIPAM-*co*-*β*-CD-AC. In addition, the ester group peak at 1718 cm^{-1} in *β*-CD-AC also appeared in PNIPAM-*co*-*β*-CD-AC. The peaks at 1420 cm^{-1} (C−O) were attenuated in PNIPAM-*co*-*β*-CD-AC. All of the above clues indicated that *β*-CD-AC and NIPAM copolymerized. The modified polysaccharides reduce the critical transition temperature and the rate of transition of temperature-sensitive hydrogels to benefit use in wounds.

X-ray photoelectron spectra (XPS) were further used to examine the surface elemental information of materials. The XPS spectra of *β*-CD, *β*-CD-AC, and PNIPAM-*co*-*β*-CD-AC are shown in Figure 1b. N 1s peaks from the NIPAM appeared in the spectrum of PNIPAM-*co*-*β*-CD-AC but not in *β*-CD and *β*-CD-AC.[35] Compared to Figure 1c,1d, it is found that the acylation of *β*-CD caused the change of the covalent bond peak. The peak at 285.5 eV was assigned to the C−OH vibrational frequency of *β*-CD[36] so that the proportion of C−OH in the grafted *β*-CD decreased to 13.8 from 62.72% of the nongrafted one. In addition, C═O and O═C−O peaks appeared at 285.3 and 288.7 eV in Figure 1d after acylation. The PNIPAM-*co*-*β*-CD-AC hydrogel was prepared by the copolymerization of *β*-CD-AC, NIPAM, and a small amount of AA. As shown in Figure 1c−f, there are C═C peaks (around 284 eV) in both *β*-CD-AC and NIPAM (Figure 1d,f), while only C═O and C−C peaks exist in the PNIPAM-*co*-*β*-CD-AC hydrogel (Figure 1f) and N 1 s (N−H) peaks of the gel in Figure 1g.[37] The above spectra data show that all monomers for the PNIPAM-*co*-*β*-CD-AC hydrogel were fully copolymerized. This result is consistent with the foregoing FTIR analysis and is similar to the previous results of the same type of paper,[36,38] which indicated the performance of a cross-linking reaction between NIPAM and *β*-CD-AC.

Acryloylated *β*-CDs are formed by the reaction of acryloyl chloride with the hydroxyl group in *β*-CD. According to the

https://doi.org/10.1021/acs.biomac.3c00708
Biomacromolecules XXXX, XXX, XXX−XXX

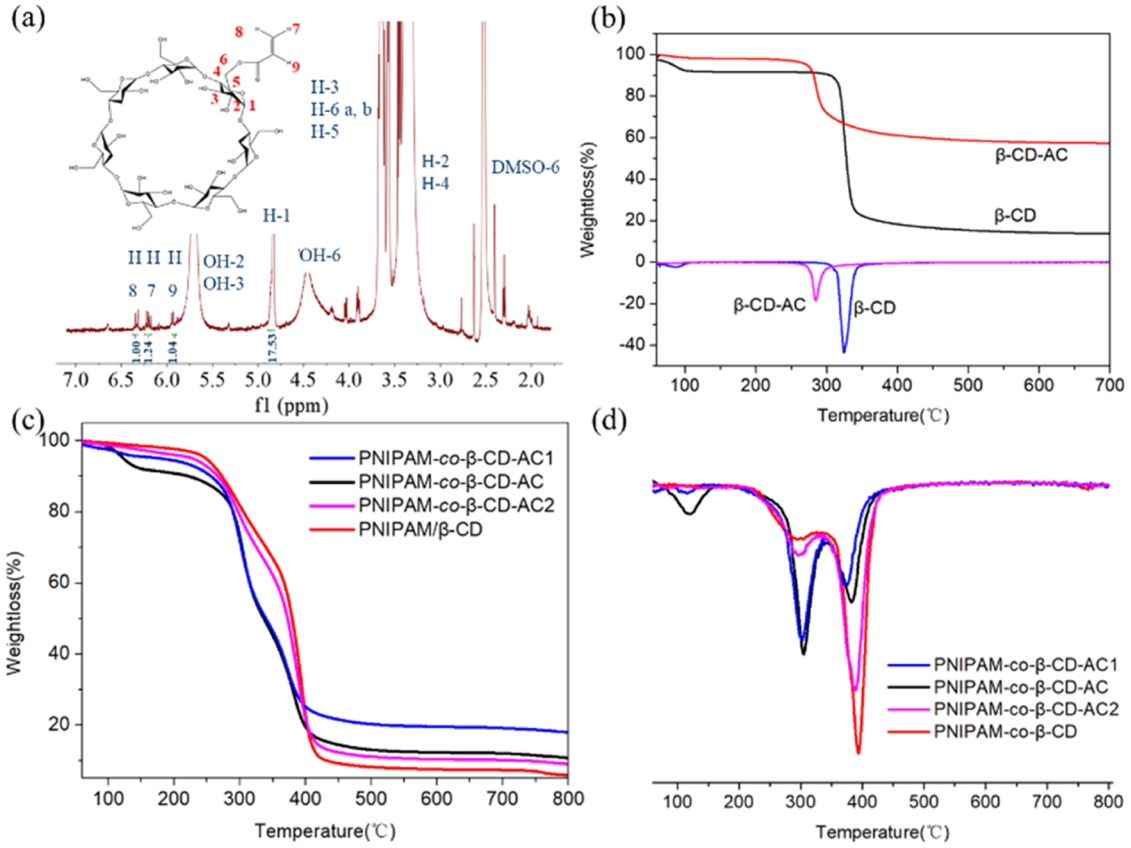

Figure 2. (a) H^1NMR spectrum of *β*-CD-AC; (b) TG and DTG curves of *β*-CD-AC and (c) *β*-CD TG and (d) DTG curves of PNIPAM/*β*-CD and PNIPAM-*co*-*β*-CD-AC in different proportions (NIPAM: *β*-CD-AC).

literature, the hydroxyl reactivities of C-2, C-3, and C-6 of glucose units in *β*-CD are different. The hydroxyl group (C-6) possesses the most vigorous reaction activity, while the hydroxyl groups (C-2, C-3) are weaker. In *β*-CD, C6-OH is located on the main face of the truncated cone-like structure and does not participate in the formation of intramolecular hydrogen bonds. The C2-OH and C3-OH between the adjacent two glucose units on the second surface can form intramolecular hydrogen bonds, showing a relatively rigid structure, so that *β*-CD has only a low solubility in aqueous solution.[39] However, in substituted *β*-CD, these hydrogen bonds no longer occur; the hydroxyl groups on C-2 and C-3 can interact with solvent water molecules. These interactions cause an increase in solubility and allow the *β*-CD to be grafted polymer from other monomers.[40]

In addition, the carbon−carbon double bond is grafted to *β*-CD by acrylation. The structure of the modified *β*-CD is identified in Figure 2a. Three signals in δ 6.0−6.5 ppm belong to H-7, H-8, and H-9 in the double bond. The degree of substitution of *β*-CD can be calculated using the following method: First, the sum (A) of the areas of the 3 vinyl protons on the double bond was obtained and then the total peak area (B at δ 4.7 ppm) of the 7 H-1 protons on the *β*-CD molecule was obtained. Finally, the average number of double bonds on each *β*-CD molecule is calculated by (A/3)/(B/7), or (7A/3B) so that the degree of substitution is calculated at 0.5. The degree of substitution of cyclodextrin fully substituted is around 1. It may be adjusted by changing the reaction conditions.[32,41] The *β*-CD-AC with 0.5° of substitution undergoes a free radical polymerization reaction with acrylic acid and NIPAM to form a hydrogel network. In addition, PEG, as a polymer molecular chain containing a large number of hydroxyl groups as shown in Scheme. 1, can form an interpenetrating network with the above hydrogel and further physically cross-link the hydrogel to give it good stability.

The thermal stability of *β*-CD, *β*-CD-AC, and PNIPAM-*co*-*β*-CD-AC hydrogels with different ratios was analyzed by TGA and DTG in Figure 2b−e. Thus, the thermal stability changes after gel copolymerization, the influence of acryloyl-*β*-CD on the gel, and the influence of different copolymerization ratios on the gel were observed. It is found that there is little weight loss (first stage) for all samples at 100 °C due to the volatilization of water, the same as in other thermogravimetric tests. The second stage between 100 and 300 °C was the decomposition of *β*-CD and the cleavage of the polymer bonds. The third stage from 294 to 394 °C was the main decomposition of NIPAM. As the ratio of *β*-CD-AC was larger, the initial decomposition temperature and maximum decomposition temperature (T_{max}) of the hydrogel were less. As shown in Table. 2, the decomposition temperature of *β*-CD-AC was lower than that of *β*-CD.

It was noticed that the PNIPAM-*co*-*β*-CD-AC hydrogel displayed good thermal stability. Since the prepared product was applied at the physiological temperature, the decomposition at a high temperature was not significant. From the above experimental data (Figure 2b−d), it was shown that the PNIPAM-*co*-*β*-CD-AC hydrogel remained stable at standard autoclave sterilization temperatures. Therefore, the PNIPAM-*co*-*β*-CD-AC hydrogel dressing could be sterilized by autoclaving before being applied to the wound site.

https://doi.org/10.1021/acs.biomac.3c00708
Biomacromolecules XXXX, XXX, XXX−XXX

Table 2. T_{max} and Weight Loss Rate of the Samples

sample name	T_{max}, °C	relative weight loss, %
β-CD	324	74.75
β-CD-AC	288	36.45
PNIPAM-*co*-β-CD-AC	305 384	73.57
PNIPAM-*co*-β-CD-AC1	294 372	69.67
PNIPAM-*co*-β-CD-AC2	302 389	75.64
PNIPAM/β-CD	296 394	80.l6

3.2. Structure and Morphologies of the PNIPAM-*co*-β-CD-AC Hydrogel. The internal structure of PNIPAM-*co*-β-CD-AC could be observed by a scanning electron microscope (SEM) after air-drying or freeze-drying, as shown in Figure 3a,b, respectively. The microporous structure of the PNIPAM-*co*-β-CD-AC hydrogel was uniform, and the hydrogel is interconnected after freeze-drying. The pore size distribution ranged from 0.8 to 1.2 μm. The porous microstructure in the PNIPAM-*co*-β-CD-AC hydrogel is beneficial to drug swell and drug release.[31] Figure S2a−c shows the automatic detection of the elements C, N, and O. This is confirmed by the overlap of the mapped spectra of these three elements, which form a joint compound. As mentioned in other papers, this interconnected porous structure facilitates wound repair by rapidly absorbing tissue secretions and blood, transporting nutrients and oxygen between pores, and promoting cellular distribution and tissue growth in them.[42] In addition, the PNIPAM-*co*-β-CD-AC hydrogel has good water vapor permeability, effectively promoting wound healing.

The dynamic rheological behavior of hydrogels was characterized by a rheometer. In general, traditional hydrogel phases are characterized by storage modulus (G') higher than loss modulus (G''). In Figure 3c, it is found that the loss modulus G'' in the low-strain region was significantly smaller than G', which indicated the existence of the hydrogel network structure. In addition, G' of PNIPAM-*co*-β-CD-AC is about 120,000 Pa, while G' of PNIPAM/β-CD is only 23,000 Pa. The difference between the two is about 5−6 times, so the former has a significant advantage in mechanical strength. The main reason is that PNIPAM/β-CD is formed by the physical cross-linking of β-CD with segments of polymer chains (copolymers of NIPAM and AA monomers). PNIPAM-*co*-β-CD-AC was formed by AA and NIPAM, and the chemical cross-linking and physical cross-linking together have greater mechanical strength.

To determine the viscoelasticity and LVE limits of the samples, a method was used to perform strain scans over a strain range of 1−200%. As shown in Figure 3d, the G' values of the samples were all higher than their respective G'' values, and the viscoelastic group of the PNIPAM-*co*-β-CD-AC hydrogel was higher than the PNIPAM/β-CD group, which had a collapse strain of 72.3%. The results indicated that after the free radical polymerization and the introduction of polymers, the intermolecular interactions and interchain entanglement were improved, resulting in a more pronounced gelation and higher mechanical strength of the hydrogels. With the increase of strain, the whole strain curve can be divided into two regions, which are the LVE region, where the strain is less than 3.75% and the G' and G'' values remain unchanged, and the *n*-LVE region, where the G' and G'' values start to change after the strain exceeds 3.75%. This indicates that 3.75% is the starting point of intermolecular chain untwisting in the PNIPAM-*co*-β-CD-AC hydrogel. In addition, the PNIPAM-*co*-β-CD-AC hydrogel exhibits significant shear-thinning behavior, suggesting that it is readily absorbed into the skin and suitable for tissue application.[31,43]

Unlike hydrogels, which generally suffer from slow temperature response, they have the high-quality properties of the 2−10 s transition state (Supporting Information Video.1). It can be seen from Figure 3c that the PNIPAM-*co*-β-CD-AC hydrogel can rapidly change from a liquid state to a gel state

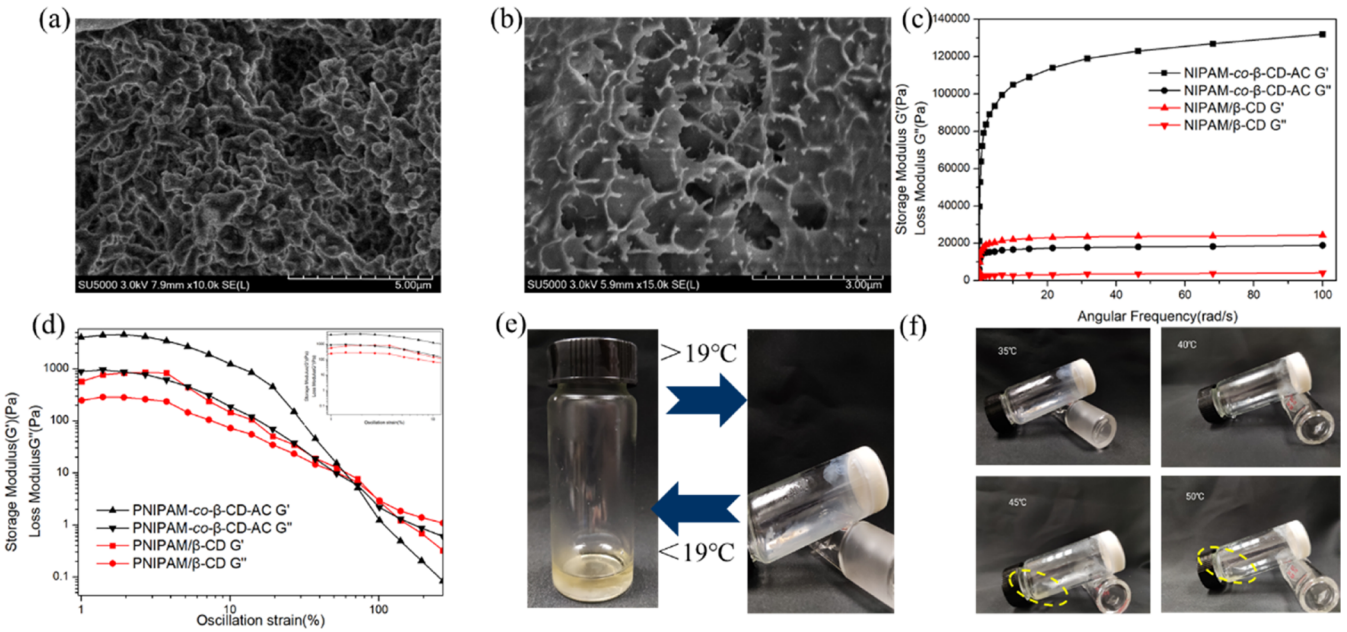

Figure 3. (a) SEM image of the hydrogel under natural drying, scale bar: 5 μm; (b) SEM image of the hydrogel under freeze-drying, scale bar: 3 μm; (c) frequency-dependent rheology measurement of PNIPAM-*co*-β-CD-AC and PNIPAM/β-CD; (d) oscillation strain rheology measurement of PNIPAM-*co*-β-CD-AC and PNIPAM/β-CD; (e) digital images of PNIPAM-*co*-β-CD-AC before and after gelation; and (f) extrusion of water from hydrogels at different temperatures.

https://doi.org/10.1021/acs.biomac.3c00708
Biomacromolecules XXXX, XXX, XXX−XXX

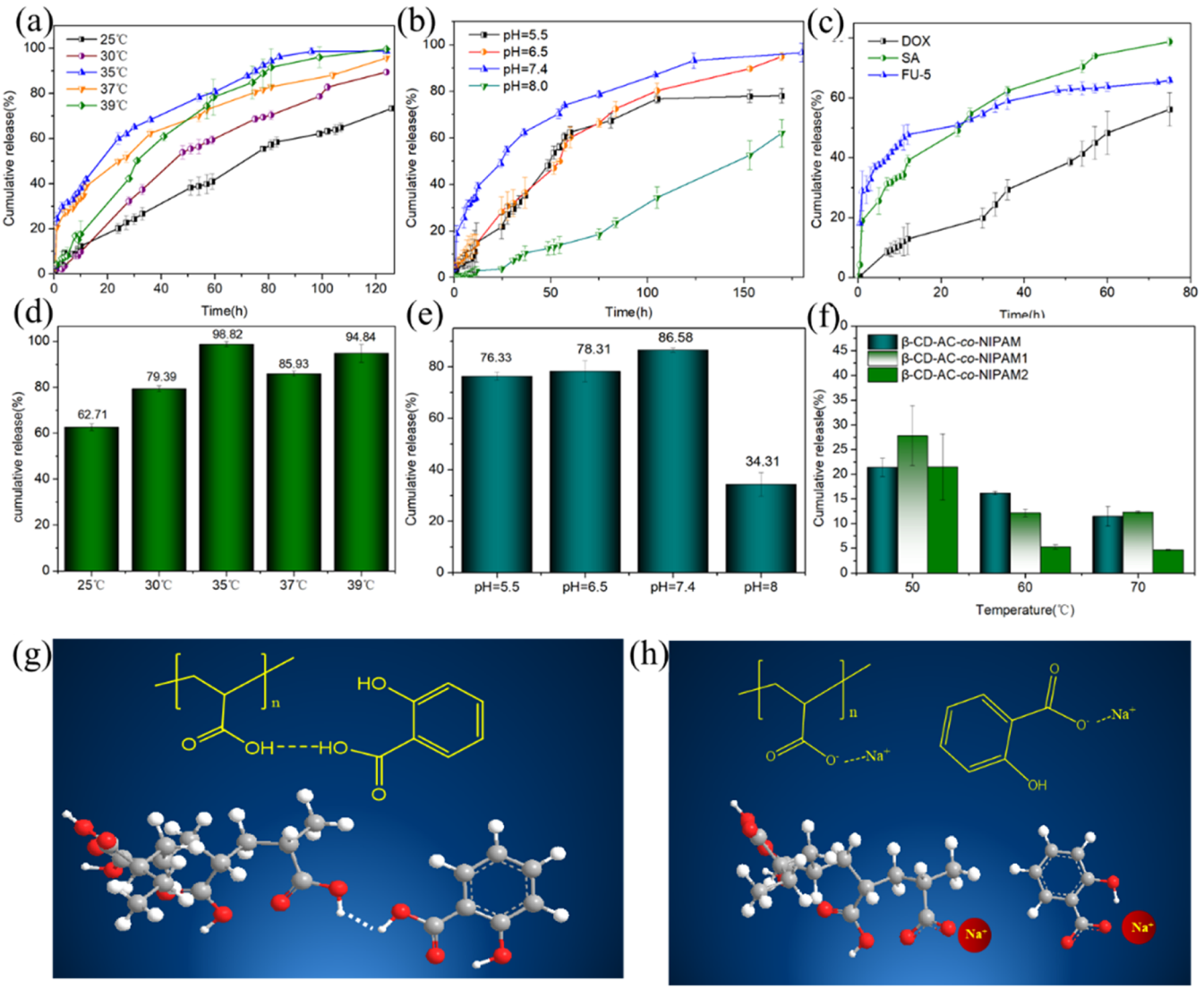

Figure 4. (a) Release amount of SA at different temperatures (%), (b) release amount of SA at different pH (%), (c) comparison of sustained release of SA, 5-Fu, and DOX at 37 °C, (d) the amount of SA released at different temperatures at 100 h (%), (e) release amount of SA at different pH at 100 h, (f) drug release of PNIPAM-*co*-*β*-CD-AC, PNIPAM-*co*-*β*-CD-AC1, and PNIPAM-*co*-*β*-CD-AC2 gels at different temperatures (50, 60, 70 °C) after 1.5 h, pH, 7.4, and (g, h) changes of PAA and SA at different pH.

when the temperature is above 19 °C. When the temperature was lower than 19 °C, the gel turned into a liquid state again. Therefore, the dressing hydrogel (PNIPAM-*co*-*β*-CD-AC) can be converted to a liquid by appropriate cooling to complete the wound dressing work. This operation can avoid secondary damage caused by traditional dressings. This is a great application prospect in wound regeneration.

Since the graft chains are in the expanded state when the temperature is lower than the LCST of the graft copolymer, they contract when the temperature is higher than the LCST. As shown in Figure 3d, the gel starts to shrink to extrude water from the gel only after it is well above the normal body temperature (40−45 °C), so it can be used normally in the wound.

3.3. Drug Release In Vitro. PNIPAM-*co*-*β*-CD-AC hydrogel will be applied to the skin surface as a wound dressing. To test the thermosensitive properties of the gels, the gels were placed in PBS buffer pH 7.4 at 25, 30, 35, 37, and 39 °C for a sustained release experiment. The simulation was performed in the temperature range that the wound might encounter. Figure 4a,d shows that the cumulative drug release at each temperature was relatively good. Furthermore, the order of cumulative release for each temperature was roughly 35 > 39 > 37 > 30 > 25 °C. After 100 h of sustained release, the cumulative release amount of SA reached the maximum. The cumulative release amount reached 98.82% at 35 °C for 105 h. At the same time, it could reach 85.93% under body temperature (37 °C), which showed that it had a good sustained release effect. This might be because the PNIPAM segments in the PNIPAM-*co*-*β*-CD-AC hydrogel begin to shrink as the temperature increases. When the gel temperature was 35 °C, the polymer chains were relatively stretched. At this time, PNIPAM was in an open state with respect to the drug contained in cyclodextrin. Therefore, the diffusion rate of molecular motion was faster at this temperature. In contrast, the pore size shrinkage of the PNIPAM-*co*-*β*-CD-AC hydrogel was more severe at 37 and 39 °C, so the release of drug molecules was reduced. In addition, at 39 °C, some SA molecules may be oxidized and decomposed due to high temperatures, which may reduce the cumulative release. At 25

https://doi.org/10.1021/acs.biomac.3c00708
Biomacromolecules XXXX, XXX, XXX−XXX

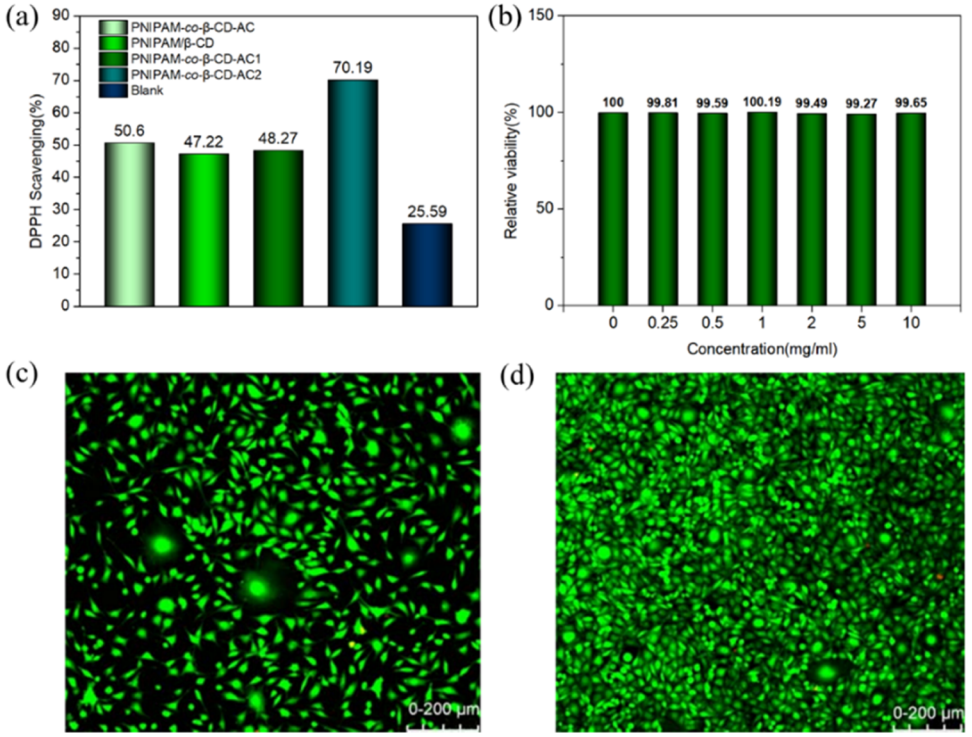

Figure 5. (a) Antioxidant activity of PNIPAM/*β*-CD and PNIPAM-*co*-*β*-CD-AC samples with different NIPAM and *β*-CD contents at specified time intervals. (b) Cell viability % of different concentrations of the tested PNIPAM-*co*-*β*-CD-AC hydrogel on L-929 cell lines after 24 h incubation. Each point was the mean ± SD (standard deviation) of three independent experiments performed in triplicate. (c) Fluorescence images of live/dead cells and (d) blank control group.

and 30 °C, the temperature was too low, resulting in a slower molecular diffusion and a smaller cumulative release.

To prove this speculation, we added a set of experiments to the drug release experiments of PNIPAM-*co*-*β*-CD-AC, PNIPAM-*co*-*β*-CD-AC1, and PNIPAM-*co*-*β*-CD-AC2 gels at 50, 60, and 70 °C. From Figure 4f, it can be seen that at 1.5 h, the gel release rate decreased with the increase in temperature. This proves that gel shrinkage at high temperatures reduces the release of a drug. In addition, it can be seen from the graph that as the proportion of *β*-CDAC in the gel increases, the SA release decreases, which is due to the subsequent increase in the level of drug encapsulation in the presence of cyclodextrin.

Because the PNIPAM-*co*-*β*-CD-AC gel was formed by the copolymerization of AA, NIPAM, and *β*-CD-AC, therefore, by adjusting the pH of PBS to simulate the pH range of wound healing (pH 5.5, 6.5, 7.4, 8), drug release experiments were performed. The results are shown in Figure 4b,e, where the release rate reached the maximum at pH 7.4 (86.57 ± 0.86% at 100 h), while the cumulative release was slightly lower at lower pH environments (pH 5, 6). In addition, since SA was an acidic substance, when pH = 8, the drug became salicylate (such as sodium salicylate), so the cumulative release was the lowest.

There are two possible causes of the above situation. The first reason was that the PNIPAM-*co*-*β*-CD-AC hydrogel contains a certain amount of carboxyl groups, as shown in Figure 4g, at high pH, carboxyl groups were converted into carboxyl anions, which led to the dissociation of hydrogen bonds between macromolecular segments due to electrostatic repulsion between anions. Therefore, the PNIPAM-*co*-*β*-CD-AC hydrogel network became loose and swollen. As mentioned in Hossein's paper,[44] the swelling amount of F-MH gel reached its maximum at pH 7.4. At this pH value, the swelling amount of the PNIPAM-*co*-*β*-CD-AC hydrogel increased, increasing the pore size of the hydrogel; therefore, the drug contained in the cyclodextrin was more likely to overflow, thereby promoting the release of drug molecules. At low pH, the carboxyl anion became a carboxyl group again, and many hydrogen bonds caused the PNIPAM-*co*-*β*-CD-AC hydrogel to show a tight shrinkage state. The SA in the gel was trapped in the cyclodextrin cavity and the polymer segment, so the release of SA is less.

The second reason was that there were mutually attractive hydrogen bonds in both the PAA fragment in the gel and the carboxyl group of SA when the pH was low. The ionization of the carboxyl group occurred when the pH increased, resulting in a decrease in the pinning force between the polymer fragments and SA.[45]

To understand the sustained release effect of other hydrophobic drugs in this gel, 5-Fu and DOX were introduced as drug models. The sustained release rule similar to SA can be seen in Figure S1a,b. As depicted in Figure 4c, all three drugs had slow-release characteristics. Therefore, the PNIPAM-*co*-*β*-CD-AC hydrogel had good drug loading and drug-releasing ability in the sustained release of hydrophobic drugs, showing the potential in wound dressing.

3.4. Antioxidative Activity and Cytotoxicity Evaluation. As the most active reactive oxygen species (ROS), hydroxyl radicals readily react with the majority of biomolecules and thus cause tissue damage or cell death.[46] Therefore, hydroxyl radicals must be further removed during the wound healing process. The antioxidant activity was determined by the DPPH radical scavenging value. The antioxidant activity of gels with different proportions

https://doi.org/10.1021/acs.biomac.3c00708
Biomacromolecules XXXX, XXX, XXX−XXX

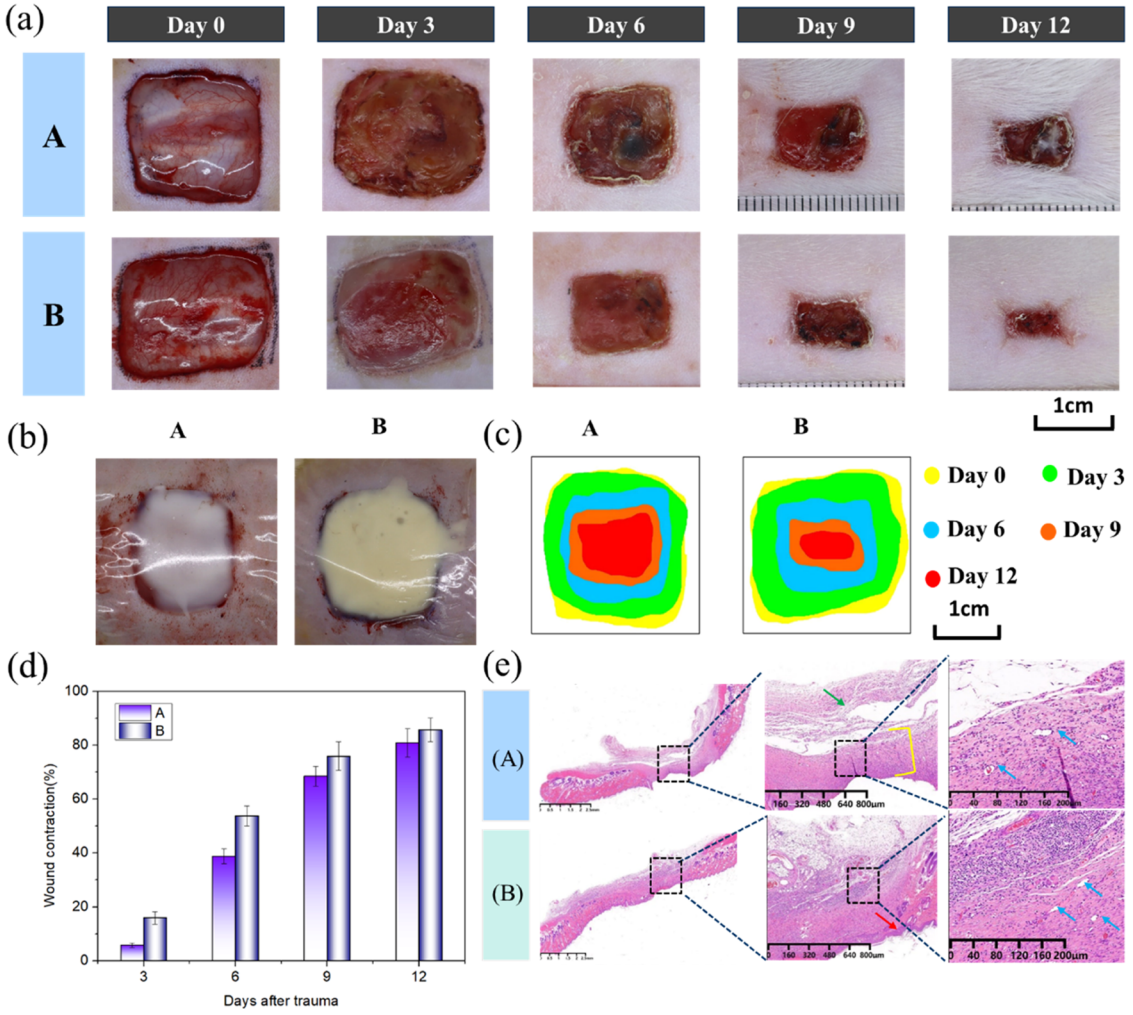

Figure 6. (a) Photos of the wound sites treated with different dressings on days 0, 3, 6, 9, and 12 after surgery and changes in wound area under different dressings (A = blank hydrogel, B = drug loading hydrogel). (b) Photos of two hydrogel groups applied to a rat wound. (c) Changes in the wound recovery area of mice at days 0, 3, 6, 9, and 12. (d) Wound healing rates of mice were calculated from the wound recovery area treated with a control group and the group of drug-loading hydrogel dressing. (e) Histomorphological evaluation of wound regeneration for (A) blank hydrogel and (B) drug loading hydrogel. The red arrow is the epithelium, the blue arrow is the neovascular, the green arrow is the connective tissue, and the yellow parentheses are granulation tissue.

(NIPAM/*β*-CD-AC = 1:1, 1:2, 2:1), PNIPAM-*co*-*β*-CD, and the control group was tested. As shown in Figure 5a, the hydrogels had the ability for DPPH scavenging in this study. The DPPH scavenging activity of hydrogels increased with the increase of the proportion of NIPAM, ranging from 48.27 to 70.19%. DPPH scavenging activity in the experimental group was significantly higher than that in the control group. In conclusion, the above results indicate that the PNIPAM-*co*-*β*-CD-AC hydrogel has a good antioxidant capacity and is potentially valuable in clinical wound dressing applications.

Considering that the PNIPAM-*co*-*β*-CD-AC hydrogel was expected to be used in the medical field, the determination of the cytotoxicity was necessary. The CCK-8 and Calcein-AM/PI staining methods evaluated the cytotoxicity of different concentrations of PNIPAM-*co*-*β*-CD-AC hydrogel aqueous extracts (Figure 5b). From Figure 5c, L-929 cells showed excellent cell activity after coculture with 10 mg/mL gel extract for 24 h. Under a confocal laser microscope, L-929 cells were filled with living cells (green fluorescence spot), and almost no dead cells could be seen (red fluorescence spot). The cytotoxicity of L-929 cells was compared with that of the control group in the medium without any additives (survival rate set at 100%), and the blank control group (Figure 5d) showed sporadic dead cells.

Figure 5b further confirms the survival rate of L-929 cells from a quantitative perspective. The survival rate of L-929 cells was higher than 99% after coculture with 0, 0.25, 0.5, 1, 2, 5, and 10 mg/mL extracted for 24 h, and even effective proliferation occurred after coculture with the extract. Compared to other scholars, hydrogels with a cell survival rate greater than 80% are considered to have better cytocompatibility.[38,47] Therefore, the above phenomenon fully proved that the PNIPAM-*co*-*β*-CD-AC hydrogel prepared had excellent cellular compatibility, which made the PNIPAM-*co*-*β*-CD-AC hydrogel have great application potential in drug sustained release and medical dressing.

3.5. Wound Healing Efficiency. To study the effects of the PNIPAM-*co*-*β*-CD-AC hydrogel dressing on wound recovery, a circular full-thickness wound was established on the back of the rat spine. To assess wound healing efficiency, we applied two different dressings to full-thickness skin wounds of 5-week-old mice. The wound dressings of mice

https://doi.org/10.1021/acs.biomac.3c00708
Biomacromolecules XXXX, XXX, XXX−XXX

are shown in Figure 6b. Figure 6a shows pictures of wound closure of the mice at different times during the 12-day treatment period. It was found that from day 3 to day 12, wound healing was much better in the drug-loaded hydrogel group than in the control group. On day 9, significant tissue atrophy could be found in the hydrogel group loaded with the drug, while the wound area in the control group remained large. The efficiency of wound recovery was calculated based on the area of the wound (Figure 6c,d). This method can be used to visualize the rate of wound recovery and the degree of healing integrity within 12 days.

Compared with blank hydrogels, the rate of wound recovery was faster with medicated hydrogels due to the presence of drugs. Histomorphometry measurements of wound regeneration on day 12 were performed by H&E staining. Wound regeneration was evaluated by observing wound re-epithelialization, migration of fibroblasts, synthesis of connective tissue, and infiltration of inflammatory cells (Figure 6e). The tight affinity between the newly formed dermis and epidermis in the drug-laden group was close to the level of wound healing of the same type of hydrogel dressing.[46] Wounds in the drug-laden group were almost healed and covered by new epithelial tissue, similar to normal skin but not in the control group. Compared with the control group, the thickness and integrity of the epidermal tissue increased in the drug-loading group. The drug-loaded hydrogel dressings effectively inhibited the infiltration of inflammatory cells. In addition, a great deal of neovascularization was observed in both groups. Connective tissue alignment and epithelial cell regeneration in the control group (blank hydrogel) were also less regular than those in the dressing group (drug-loaded). The control group performed slightly better compared to the control group in other papers of the same type,[46,48] but there was very thin and incomplete skin. This may be because the hydrogel itself has good biocompatibility and high water retention. The wound recovers better in a moist environment.[49] As shown in Figure 6e, the drug-laden hydrogel showed good results in wound repair, rapid regenerative epithelialization, inhibition of inflammation, and connective tissue remodeling. This ability to promote wound repair is mainly attributed to the histocompatibility, antioxidant activity, moisturizing properties, and appropriate surface microstructure of the PNIPAM-co-β-CD-AC hydrogel.[50]

4. CONCLUSIONS

A new ultralow temperature thermosensitive supramolecular hydrogel was prepared by copolymerizing NIPAM, β-CD-AC, and AA for sustained drug release in wound dressings. In the presence of cyclodextrins, the sustained release effect of hydrophobic drugs such as SA was facilitated due to their host−guest interaction. The copolymerization of NIPAM and hydrophilic fragments on β-CD increased the temperature-sensitive and fast critical phase transition rate of the hydrogel so that the gel can be used as a wound dressing to quickly fit on irregular wounds. The β-CD-AC-grafted PNIPAM prefers to reduce the LCST, which is lower than that of pure PNIPAM, making such hydrogel dressings stable on the skin surface at low temperatures. With noncytotoxicity, antioxidants, and sustained drug release, the synthesized NIPAM-co-β-CD-ACs have great potential for applications in the biomedical field, such as wound dressings.

ASSOCIATED CONTENT

Supporting Information

The Supporting Information is available free of charge at https://pubs.acs.org/doi/10.1021/acs.biomac.3c00708.

Videos of NIPAM-co-β-CD-AC before and after gelation; release amount of 5-FU at different temperatures (%); release amount of DOX at different temperatures (%); and EDX spectra of NIPAM-co-β-CD-AC (PDF)

AUTHOR INFORMATION

Corresponding Author

Shiyu Fu − *State Key Laboratory of Pulp and Paper Engineering, South China University of Technology, Guangzhou 510640, China;* orcid.org/0000-0001-5680-7493; Phone: +8613570017263; Email: shyfu@scut.edu.cn

Authors

Juanli Shen − *State Key Laboratory of Pulp and Paper Engineering, South China University of Technology, Guangzhou 510640, China;* orcid.org/0000-0002-5701-6826

Xiaohong Liu − *State Key Laboratory of Pulp and Paper Engineering, South China University of Technology, Guangzhou 510640, China*

Shenglong Tian − *State Key Laboratory of Pulp and Paper Engineering, South China University of Technology, Guangzhou 510640, China;* orcid.org/0000-0002-3436-1336

Detao Liu − *State Key Laboratory of Pulp and Paper Engineering, South China University of Technology, Guangzhou 510640, China*

Hao Liu − *State Key Laboratory of Pulp and Paper Engineering, South China University of Technology, Guangzhou 510640, China*

Complete contact information is available at: https://pubs.acs.org/10.1021/acs.biomac.3c00708

Notes

The authors declare no competing financial interest.

ACKNOWLEDGMENTS

This work was supported by the National Key Research and Development Program (2021YFE0104500), the National Natural Science Foundation of China (22078114), the Natural Science Foundation of Guangdong Province (2021A1515010285), and the Key Research and Development Program of Guangzhou Science and Technology Program (202103000011). The authors would like to Shiyanjia Lab (www.shiyanjia.com) for the XPS analysis.

REFERENCES

(1) (a) Karino, T.; Shibayama, M.; Okumura, Y.; Ito, K. SANS study on pulley effect of slide-ring gel. *Phys. B* **2006**, *385*−*386*, 807−809. (b) Zhang, M.; Xiong, Q.; Wang, Y.; Zhang, Z.; Shen, W.; Liu, L.; Wang, Q.; Zhang, Q. A well-defined coil−comb polycationic brush with "star polymers" as side chains for gene delivery. *Polym. Chem.* **2014**, *5* (16), 4670−4678.

(2) Wu, Y.; Qi, H.; Shi, C.; Ma, R.; Liu, S.; Huang, Z. Preparation and adsorption behaviors of sodium alginate-based adsorbent-immobilized β-cyclodextrin and graphene oxide. *RSC Adv.* **2017**, *7* (50), 31549−31557.

(3) Li, R.; Zhang, X.; Zhang, Q.; Liu, H.; Rong, J.; Tu, M.; Zeng, R.; Zhao, J. β-cyclodextrin-conjugated hyaluronan hydrogel as a potential drug sustained delivery carrier for wound healing. *J. Appl. Polym. Sci.* **2016**, *133* (9), No. 43072.
(4) Zhang, L.; Zhou, J.; Zhang, L. Structure and properties of beta-cyclodextrin/cellulose hydrogels prepared in NaOH/urea aqueous solution. *Carbohydr. Polym.* **2013**, *94* (1), 386−393.
(5) (a) Chen, D.; Ren, G.; Zhao, X.; Luo, J.; Wang, H.; Jia, P. A cyclodextrin-phenylboronic acid cross-linked hydrogel with drug hosting, self-healing and pH-sensitive properties for sustained drug release. *New J. Chem.* **2021**, *45* (24), 10711−10717. (b) Zhang, J. T.; Huang, S. W.; Xue, Y. N.; Liu, J.; Zhuo, R. X. Thermal-sensitive beta-cyclodextin-containing poly(N-isopropylacrylamide) hydrogels cross-linked by Si-o-Si bonds-synthesis, charactrization and prolonging in vitro release of 5-Fluorouracil. *Chin. J. Polym. Sci.* **2005**, *23* (05), 513−519.
(6) Lou, C.; Tian, X.; Deng, H.; Wang, Y.; Jiang, X. Dialdehyde-beta-cyclodextrin-crosslinked carboxymethyl chitosan hydrogel for drug release. *Carbohydr. Polym.* **2020**, *231*, No. 115678.
(7) Sugawara, A.; Asoh, T.-A.; Takashima, Y.; Harada, A.; Uyama, H. Composite hydrogels reinforced by cellulose-based supramolecular filler. *Polym. Degrad. Stab.* **2020**, *177*, No. 109157.
(8) (a) Song, X.; Zhang, Z.; Zhu, J.; Wen, Y.; Zhao, F.; Lei, L.; Phan-Thien, N.; Khoo, B. C.; Li, J. Thermoresponsive Hydrogel Induced by Dual Supramolecular Assemblies and Its Controlled Release Property for Enhanced Anticancer Drug Delivery. *Biomacromolecules* **2020**, *21* (4), 1516−1527. (b) Przybyla, M. A.; Yilmaz, G.; Becer, C. R. Natural cyclodextrins and their derivatives for polymer synthesis. *Polym. Chem.* **2020**, *11* (48), 7582−7602.
(9) Zhou, H. Y.; Wang, Z. Y.; Duan, X. Y.; Jiang, L. J.; Cao, P. P.; Li, J. X.; Li, J. B. Design and evaluation of chitosan-β-cyclodextrin based thermosensitive hydrogel. *Biochem. Eng. J.* **2016**, *111*, 100−107.
(10) Tang, L.; Wang, L.; Yang, X.; Feng, Y.; Li, Y.; Feng, W. Poly(N-isopropylacrylamide)-based smart hydrogels: Design, properties and applications. *Prog. Mater. Sci.* **2021**, *115*, No. 100702.
(11) Yang, L.-l.; Zhang, J.-m.; He, J.-s.; Zhang, J.; Gan, Z.-h. Synthesis and characterization of temperature-sensitive cellulose-graft-poly(N-isopropylacrylamide) copolymers. *Chin. J. Polym. Sci.* **2015**, *33* (12), 1640−1649.
(12) (a) Crini, G.; Fenyvesi, É; Szente, L. Outstanding contribution of Professor József Szejtli to cyclodextrin applications in foods, cosmetics, drugs, chromatography and biotechnology: a review. *Environ. Chem. Lett.* **2021**, *19* (3), 2619−2641. (b) Diaz-Salmeron, R.; Toussaint, B.; Huang, N.; Ducournau, E. B.; Alviset, G.; Dufay, S. G.; Hillaireau, H.; Wojcicki, A. D.; Boudy, V. Mucoadhesive Poloxamer-Based Hydrogels for the Release of HP-beta-CD-Complexed Dexamethasone in the Treatment of Buccal Diseases. *Pharmaceutics* **2021**, *13* (1), No. 117, DOI: 10.3390/pharmaceutics13010117.
(13) Deng, Z.; Guo, Y.; Zhao, X.; Ma, P. X.; Guo, B. Multifunctional Stimuli-Responsive Hydrogels with Self-Healing, High Conductivity, and Rapid Recovery through Host−Guest Interactions. *Chem. Mater.* **2018**, *30* (5), 1729−1742.
(14) Miao, F.; Li, Y.; Tai, Z.; Zhang, Y.; Gao, Y.; Hu, M.; Zhu, Q. Antimicrobial Peptides: The Promising Therapeutics for Cutaneous Wound Healing. *Macromol. Biosci.* **2021**, *21* (10), No. 2100103.
(15) Zhang, S.; Shan, S.; Zhang, H.; Gao, X.; Tang, X.; Chen, K. Antimicrobial cellulose hydrogels preparation with RIF loading from bamboo parenchyma cells: A green approach towards wound healing. *Int. J. Biol. Macromol.* **2022**, *203*, 1−9.
(16) Peng, W.; Li, D.; Dai, K.; Wang, Y.; Song, P.; Li, H.; Tang, P.; Zhang, Z.; Li, Z.; Zhou, Y.; Zhou, C. Recent progress of collagen, chitosan, alginate and other hydrogels in skin repair and wound dressing applications. *Int. J. Biol. Macromol.* **2022**, *208*, 400−408.
(17) Hao, R.; Cui, Z.; Zhang, X.; Tian, M.; Zhang, L.; Rao, F.; Xue, J. Rational Design and Preparation of Functional Hydrogels for Skin Wound Healing. *Front. Chem.* **2021**, *9*, No. 839055.
(18) (a) Cao, S.; Xu, G.; Li, Q.; Zhang, S.; Yang, Y.; Chen, J. Double crosslinking chitosan sponge with antibacterial and hemostatic properties for accelerating wound repair. *Composites, Part B* **2022**, *234*, No. 109746. (b) Shen, J.; Chang, R.; Chang, L.; Wang, Y.; Deng, K.; Wang, D.; Qin, J. Light emitting CMC-CHO based self-healing hydrogel with injectability for in vivo wound repairing applications. *Carbohydr. Polym.* **2022**, *281*, No. 119052.
(19) Huan, Y.; Kong, Q.; Tang, Q.; Wang, Y.; Mou, H.; Ying, R.; Li, C. Antimicrobial peptides/ciprofloxacin-loaded O-carboxymethyl chitosan/self-assembling peptides hydrogel dressing with sustained-release effect for enhanced anti-bacterial infection and wound healing. *Carbohydr. Polym.* **2022**, *280*, No. 119033.
(20) Alizadehgiashi, M.; Nemr, C. R.; Chekini, M.; Ramos, D. P.; Mittal, N.; Ahmed, S. U.; Khuu, N.; Kelley, S. O.; Kumacheva, E. Multifunctional 3D-Printed Wound Dressings. *ACS Nano* **2021**, *15* (7), 12375−12387.
(21) (a) Li, L.; He, Y.; Zheng, X.; Yi, L.; Nian, W. Progress on Preparation of pH/Temperature-Sensitive Intelligent Hydrogels and Applications in Target Transport and Controlled Release of Drugs. *Int. J. Polym. Sci.* **2021**, *2021*, 1−14. (b) Yang, Y.; Xu, L.; Wang, J.; Meng, Q.; Zhong, S.; Gao, Y.; Cui, X. Recent advances in polysaccharide-based self-healing hydrogels for biomedical applications. *Carbohydr. Polym.* **2022**, *283*, No. 119161.
(22) Sun, X.-Z.; Wu, J.-Z.; Wang, H.-D.; Guan, C. Thermosensitive Cotton Textile Loaded with Cyclodextrin-complexed Curcumin as a Wound Dressing. *Fibers Polym.* **2021**, *22* (9), 2475−2482.
(23) Yang, M.; Xie, R.; Wang, J.-Y.; Ju, X.-J.; Yang, L.; Chu, L.-Y. Gating characteristics of thermo-responsive and molecular-recognizable membranes based on poly(N-isopropylacrylamide) and β-cyclodextrin. *J. Membr. Sci.* **2010**, *355* (1−2), 142−150.
(24) (a) Roy, A.; Maity, P. P.; Bose, A.; Dhara, S.; Pal, S. β-Cyclodextrin based pH and thermo-responsive biopolymeric hydrogel as a dual drug carrier. *Mater. Chem. Front.* **2019**, *3* (3), 385−393. (b) López-González, M.; Melia Rodrigo, M.; Valiente, M.; Trabado, I.; Mendicuti, F.; Marcelo, G. Structuring hydrophobic domains in Poly(N-isopropylacrylamide-co-Methacrylic acid) hydrogels. *Eur. Polym. J.* **2020**, *131*, No. 109695.
(25) (a) Khorram, M.; Vasheghani-Farahani, E.; Dinarvand, R. Preparation of poly(-isopropylacrylamide) hollow beads as reservoir drug delivery systems. *J. Controlled Release* **2006**, *116* (2), e31−e33. (b) Zhang, X. Z.; Zhuo, R. X.; Cui, J. Z.; Zhang, J. T. A novel thermo-responsive drug delivery system with positive controlled release. *Int. J. Pharm.* **2002**, *235* (1−2), 43−50.
(26) Prasannan, A.; Tsai, H.-C.; Hsiue, G.-H. Formulation and evaluation of epinephrine-loaded poly(acrylic acid-co-N-isopropylacrylamide) gel for sustained ophthalmic drug delivery. *React. Funct. Polym.* **2018**, *124*, 40−47.
(27) Okudan, A.; Altay, A. Investigation of the Effects of Different Hydrophilic and Hydrophobic Comonomers on the Volume Phase Transition Temperatures and Thermal Properties of N-Isopropylacrylamide-Based Hydrogels. *Int. J. Polym. Sci.* **2019**, *2019*, 1−12.
(28) Malik, N. S.; Ahmad, M.; Minhas, M. U. Cross-linked beta-cyclodextrin and carboxymethyl cellulose hydrogels for controlled drug delivery of acyclovir. *PLoS One* **2017**, *12* (2), No. e0172727.
(29) Li, P.; Hou, X.; Qu, L.; Dai, X.; Zhang, C. PNIPAM-MAPOSS Hybrid Hydrogels with Excellent Swelling Behavior and Enhanced Mechanical Performance: Preparation and Drug Release of 5-Fluorouracil. *Polymers* **2018**, *10* (2), No. 137.
(30) Bolouki, N.; Hsu, Y. N.; Hsiao, Y. C.; Jheng, P. R.; Hsieh, J. H.; Chen, H. L.; Mansel, B. W.; Yeh, Y. Y.; Chen, Y. H.; Lu, C. X.; et al. Cold atmospheric plasma physically reinforced substances of platelets-laden photothermal-responsive methylcellulose complex restores burn wounds. *Int. J. Biol. Macromol.* **2021**, *192*, 506−515.
(31) Lin, Y. Y.; Lu, S. H.; Gao, R.; Kuo, C. H.; Chung, W. H.; Lien, W. C.; Wu, C. C.; Diao, Y.; Wang, H. D. A Novel Biocompatible Herbal Extract-Loaded Hydrogel for Acne Treatment and Repair. *Oxid. Med. Cell. Longevity* **2021**, *2021*, No. 5598291.
(32) Yu, R.; Yang, Y.; He, J.; Li, M.; Guo, B. Novel supramolecular self-healing silk fibroin-based hydrogel via host−guest interaction as wound dressing to enhance wound healing. *Chem. Eng. J.* **2021**, *417*, No. 128278.

https://doi.org/10.1021/acs.biomac.3c00708
Biomacromolecules XXXX, XXX, XXX−XXX

(33) (a) Sedghi, R.; Ashrafzadeh, S.; Heidari, B. pH-sensitive molecularly imprinted polymer based on graphene oxide for stimuli actuated controlled release of curcumin. *J. Alloys Compd.* **2021**, *857*, No. 157603. (b) Gao, Q.; Hu, J.; Shi, J.; Wu, W.; Debeli, D. K.; Pan, P.; Shan, G. Fast photothermal poly(NIPAM-co-beta-cyclodextrin) supramolecular hydrogel with self-healing through host-guest interaction for intelligent light-controlled switches. *Soft Matter* **2020**, *16* (46), 10558−10566.
(34) Sun, J.; Zhao, X.; Sun, G.; Zhao, H.; Yan, L.; Jiang, X.; Cui, Y. Phosphate-crosslinked β-cyclodextrin polymer for highly efficient removal of Pb(ii) from acidic wastewater. *New J. Chem.* **2022**, *46* (8), 3631−3639.
(35) Wang, Z.; Chen, H.; Gao, X.; Hu, B.; Meng, Q.; Zhao, C.; Yang, L.; Zheng, H. A novel self-floating cyclodextrin-modified polymer for cationic dye removal: Preparation, adsorption behavior and mechanism. *Sep. Purif. Technol.* **2022**, *290*, No. 120838.
(36) Taka, A. L.; Doyle, B. P.; Carleschi, E.; Fonkui, T. Y.; Erasmus, R.; Fosso-Kankeu, E.; Pillay, K.; Mbianda, X. Y. Spectroscopic characterization and antimicrobial activity of nanoparticle doped cyclodextrin polyurethane bionanosponge. *Mater. Sci. Eng., C* **2020**, *115*, No. 111092.
(37) Zou, Z.; Jiang, Y.; Song, K. Pd Nanoparticles Assembled on Metalporphyrin-Based Microporous Organic Polymer as Efficient Catalyst for Tandem Dehydrogenation of Ammonia Borane and Hydrogenation of Nitro Compounds. *Catal. Lett.* **2020**, *150* (5), 1277−1286.
(38) Huang, S.; Liu, H.; Liao, K.; Hu, Q.; Guo, R.; Deng, K. Functionalized GO Nanovehicles with Nitric Oxide Release and Photothermal Activity-Based Hydrogels for Bacteria-Infected Wound Healing. *ACS Appl. Mater. Interfaces* **2020**, *12* (26), 28952−28964.
(39) (a) Gattuso, G.; Nepogodiev, S. A.; Stoddart, J. F. Synthetic cyclic oligosaccharides. *Chem. Rev.* **1998**, *98* (5), 1919−1958. (b) Saenger, W. R.; Jacob, J.; Gessler, K.; Steiner, T.; Hoffmann, D.; Sanbe, H.; Koizumi, K.; Smith, S. M.; Takaha, T. Structures of the common cyclodextrins and their larger analogues - Beyond the doughnut. *Chem. Rev.* **1998**, *98* (5), 1787−1802.
(40) Constantin, M.; Bucatariu, S.; Ascenzi, P.; Simionescu, B. C.; Fundueanu, G. Poly(NIPAAm-co-beta-cyclodextrin) microgels with drug hosting and temperature-dependent delivery properties. *React. Funct. Polym.* **2014**, *84*, 1−9.
(41) Sedghi, R.; Yassari, M.; Heidari, B. Thermo-responsive molecularly imprinted polymer containing magnetic nanoparticles: Synthesis, characterization and adsorption properties for curcumin. *Colloids Surf., B* **2018**, *162*, 154−162.
(42) Zhang, W.; Zhang, Y.; Li, X.; Cao, Z.; Mo, Q.; Sheng, R.; Ling, C.; Chi, J.; Yao, Q.; Chen, J.; Wang, H. Multifunctional polyphenol-based silk hydrogel alleviates oxidative stress and enhances endogenous regeneration of osteochondral defects. *Mater. Today Bio* **2022**, *14*, No. 100251.
(43) (a) Lin, N.; Dufresne, A. Supramolecular hydrogels from in situ host-guest inclusion between chemically modified cellulose nanocrystals and cyclodextrin. *Biomacromolecules* **2013**, *14* (3), 871−880. (b) Peng, Q.; Wu, Q.; Chen, J.; Wang, T.; Wu, M.; Yang, D.; Peng, X.; Liu, J.; Zhang, H.; Zeng, H. Coacervate-Based Instant and Repeatable Underwater Adhesive with Anticancer and Antibacterial Properties. *ACS Appl. Mater. Interfaces* **2021**, *13* (40), 48239−48251. (c) Lee, H. J.; Le, P. T.; Kwon, H. J.; Park, K. D. Supramolecular assembly of tetronic−adamantane and poly(β-cyclodextrin) as injectable shear-thinning hydrogels. *J. Mater. Chem. B* **2019**, *7* (21), 3374−3382.
(44) Derakhshankhah, H.; Haghshenas, B.; Eskandani, M.; Jahanban-Esfahlan, R.; Abbasi-Maleki, S.; Jaymand, M. Folate-conjugated thermal- and pH-responsive magnetic hydrogel as a drug delivery nano-system for "smart" chemo/hyperthermia therapy of solid tumors. *Mater. Today Commun.* **2022**, *30*, No. 103148.
(45) Qiu, Y.; Park, K. Environment-sensitive hydrogels for drug delivery. *Adv. Drug Delivery Rev.* **2001**, *53* (3), 321−339.
(46) Qiu, X.; Zhang, J.; Cao, L.; Jiao, Q.; Zhou, J.; Yang, L.; Zhang, H.; Wei, Y. Antifouling Antioxidant Zwitterionic Dextran Hydrogels as Wound Dressing Materials with Excellent Healing Activities. *ACS Appl. Mater. Interfaces* **2021**, *13* (6), 7060−7069.
(47) Li, J.; Wang, Y.; Yang, J.; Liu, W. Bacteria activated-macrophage membrane-coated tough nanocomposite hydrogel with targeted photothermal antibacterial ability for infected wound healing. *Chem. Eng. J.* **2021**, *420*, No. 127638.
(48) (a) Dong, L.; Han, Z.; Zhang, H.; Yang, R.; Fang, J.; Wang, L.; Li, X.; Li, X. Tea polyphenol/glycerol-treated double-network hydrogel with enhanced mechanical stability and anti-drying, antioxidant and antibacterial properties for accelerating wound healing. *Int. J. Biol. Macromol.* **2022**, *208*, 530−543. (b) Zhang, P.; He, L.; Zhang, J.; Mei, X.; Zhang, Y.; Tian, H.; Chen, Z. Preparation of novel berberine nano-colloids for improving wound healing of diabetic rats by acting Sirt1/NF-kappaB pathway. *Colloids Surf., B* **2020**, *187*, No. 110647. (c) Liu, H.; Li, Z.; Zhao, Y.; Feng, Y.; Zvyagin, A. V.; Wang, J.; Yang, X.; Yang, B.; Lin, Q. Novel Diabetic Foot Wound Dressing Based on Multifunctional Hydrogels with Extensive Temperature-Tolerant, Durable, Adhesive, and Intrinsic Antibacterial Properties. *ACS Appl. Mater. Interfaces* **2021**, *13* (23), 26770−26781.
(49) Wang, S.; Liu, R.; Bi, S.; Zhao, X.; Zeng, G.; Li, X.; Wang, H.; Gu, J. Mussel-inspired adhesive zwitterionic composite hydrogel with antioxidant and antibacterial properties for wound healing. *Colloids Surf., B* **2022**, *220*, No. 112914.
(50) (a) Liang, Y.; He, J.; Guo, B. Functional Hydrogels as Wound Dressing to Enhance Wound Healing. *ACS Nano* **2021**, *15* (8), 12687−12722. (b) Yu, R.; Li, M.; Li, Z.; Pan, G.; Liang, Y.; Guo, B. Supramolecular Thermo-Contracting Adhesive Hydrogel with Self-Removability Simultaneously Enhancing Noninvasive Wound Closure and MRSA-Infected Wound Healing. *Adv. Healthcare Mater.* **2022**, *11* (13), No. e2102749.

https://doi.org/10.1021/acs.biomac.3c00708
Biomacromolecules XXXX, XXX, XXX−XXX